Published in final edited form as:

FEBS Lett. 2022 February ; 596(4): 417–426. doi:10.1002/1873-3468.14273.

PIP_3 abundance overcomes PI3K signaling selectivity in invadopodia

Charles T. Jakubik[1], **Claire C. Weckerly**[2], **Gerald R.V. Hammond**[2], **Anne R. Bresnick**[1,*], **Jonathan M. Backer**[1,3,*]

[1]Department of Biochemistry, Albert Einstein College of Medicine, 1300 Morris Park Avenue Bronx, NY

[2]Department of Cell Biology, University of Pittsburgh School of Medicine, Pittsburgh, PA

[3]Department of Molecular Pharmacology, Albert Einstein College of Medicine, 1300 Morris Park Avenue, Bronx, NY

Abstract

PI3Kβ is required for invadopodia-mediated matrix degradation by breast cancer cells. Invadopodia maturation requires GPCR activation of PI3Kβ and its coupling to SHIP2 to produce $PI(3,4)P_2$. We now test whether selectivity for PI3Kβ is preserved under conditions of mutational increases in PI3K activity. In breast cancer cells where PI3Kβ is inhibited, short chain diC8-PIP_3 rescues gelatin degradation in a SHIP2-dependent manner; rescue by diC8-$PI(3,4)P_2$ is SHIP2-independent. Surprisingly, expression of either activated PI3Kβ or PI3Kα mutants rescued the effects of PI3Kβ inhibition. In both cases, gelatin degradation was SHIP2-dependent. These data confirm the requirement for PIP_3 conversion to $PI(3,4)P_2$ for invadopodia function, and suggest that selectivity for distinct PI3K isotypes may be obviated by mutational activation of the PI3K pathway.

Graphical Abstract

GPCR activation of PI3Kβ drives invadopodia-mediated matrix degradation by breast cancer cells, via PI3Kβ coupling to SHIP2 to produce $PI(3,4)P_2$. Surprisingly, expression of either activated PI3Kβ or PI3Kα rescues the effects of pertussis toxin or TGX221, which inhibit PI3Kβ. In both cases, matrix degradation is SHIP2-dependent. Thus, selectivity for PI3K isotypes is obviated by mutational activation of PI3K signaling.

*To whom correspondence should be addressed: ARB: 718-430-2741, anne.bresnick@einsteinmed.edu, JMB: 718-430-2153, jonathan.backer@einsteinmed.edu.

Author Contributions:

Experimental data: C.T.J., C.C.W.; Writing and editing: C.T.J., C.C.W., G.R.V.H., A.R.B., J.M.B.; Supervision: G.R.V.H., A.R.B., J.M.B.; Funding acquisition: A.R.B., J.M.B., G.R.V.H.

Competing Interests:

The authors have no competing interests.

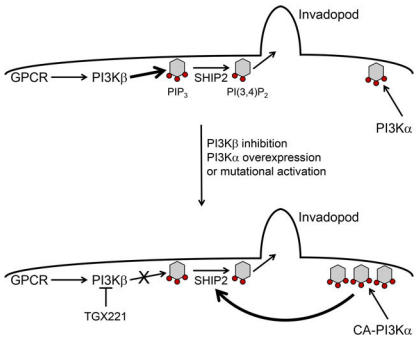

Keywords

PI 3-kinase; invadopodia; matrix degradation

Introduction

Invadopodia are protrusive structures that degrade extracellular matrix (ECM) and promote tumor cell invasion into surrounding tissue. Invadopodia are required for numerous steps in the metastatic cascade, including local invasion, intravasation, and extravasation (1,2). Invadopodia formation occurs in a step-wise manner (3). Invadopodia precursors, which cannot degrade ECM, contain a core composed of actin, the actin-binding protein cortactin, the adapter protein Tks5, and actin regulatory proteins such as N-WASP, Arp2/3, cofilin, and dynamin (3,4). Mature invadopodia contain phosphorylated cortactin and adapter proteins as well as Nck and p130Cas, and are surrounded by cell adhesion proteins including β1-integrins and paxillin (2,3,5). Mature invadopodia utilize the microtubule cytoskeleton to deliver metalloproteinases (MMPs and ADAMs) to invadopodia tips, enabling ECM degradation (3,4,6).

Class IA PI3Ks play a critical role in invadopodia maturation (7–9). Class IA PI3Ks are heterodimers containing a catalytic subunit (p110α, p110β, p110δ) bound to a regulatory subunit (p85α, p85β, p55α, p50α, p55γ), and are activated downstream of receptor tyrosine kinases (RTKs) and G protein coupled receptors (GPCRs) (10). PI3Kβ (a heterodimer containing p85 and p110β) is unique among class IA PI3Ks in that it is regulated by p85 binding to RTKs and by p110β binding to Gβγ, Rab5, Rac1, and Cdc42 (11). Upon activation, PI3Kβ is recruited to the plasma membrane leading to the production of PI(3,4,5)P_3 (PIP_3) and the recruitment of downstream effectors that contain Pleckstrin homology (PH) domains (12). PIP_3 is converted to PI(3,4)P_2 by the phosphoinositide 5′-phosphatases SHIP2 and synaptojanin-2 (SYNJ2) (13,14). The conversion of PIP_3 to PI(3,4)P_2 recruits distinct downstream effectors such as Tks5 and lamellipodin to the invadopod, which are required for invadopodia maturation (7,15).

Our lab previously showed that PI3Kβ is selectively required for invadopodia-mediated matrix degradation by MDA-MB-231, BT549 and MDA-MB-468 breast cancer cells (7,16). PI3Kβ is not required for the formation of invadopodial precursors (measured by cortactin-F-actin punctae that do not colocalize with degraded gelatin) but is required for invadopodial

maturation (measured by cortactin-F-actin punctae colocalized with gelatin degradation) (7). The selective requirement for PI3Kβ during invadopod maturation may be due in part to its involvement in integrin-stimulated responses (7), as integrin activation is required for invadopodia maturation (2,5).

The requirement for PI3Kβ for $PI(3,4)P_2$ production during integrin-stimulated invadopodia maturation is not understood, but could reflect the localization of PI3Kβ to regions of the cell that contain SHIP2. However, in cells expressing activated mutants of PI3K, it is possible that overall increases in PIP_3 production could bypass the requirement for PI3Kβ. Using short-chain soluble phosphoinositides and activated PI3Kβ and PI3Kα mutants, we show that increases in PIP_3 production are sufficient to overcome inhibition of PI3Kβ with regard to invadopodia-mediated gelatin degradation, regardless of the source of the lipids. These data have important implications for the use of PI3Kβ inhibition in tumors that express activated PI3Kα.

Results

Short chain phosphoinositides rescue gelatin degradation in PTX- or TGX221-treated MDA-MB-231 cells.

To manipulate PIP_3 levels in the cell independently of PI3Kβ localization, we used short chain phosphoinositides (di-octanoyl; C8) that can be added directly to cells to induce signaling functions (17,18). We used these lipids to bypass inhibition of PI3Kβ by pertussis toxin (PTX), which blocks GPCR activation of PI3Kβ, or by the PI3Kβ-selective kinase inhibitor TGX221. Treatment of MDA-MB-231 cells with PTX blocks gelatin degradation (Fig. 1A). However, degradation was rescued by the addition of diC8-PIP_3 or diC8-$PI(3,4)P_2$, but not diC8-$PI(3,5)P_2$. Similar results were obtained in cells treated with TGX221 (Fig. 1B).

Interestingly, PIP_3 and $PI(3,4)P_2$ showed similar potency in the rescue of gelatin degradation; dose responses showed maximal rescue at a concentration of 1 μM for both lipids (data not shown). Given that invadopodia maturation requires $PI(3,4)P_2$, this suggested that diC8-PIP_3 was efficiently converted to $PI(3,4)P_2$ during the 18 h gelatin degradation assay. We examined this in two ways. First, we used a previously described fluorescent biosensor for $PI(3,4)P_2$ to measure intracellular levels of this lipid after incubation of cells with diC8-phosphoinositides (19). Unlike acute stimulation with EGF, which produced increases in both $PI(3,4)P_2$ and PIP_3, acute stimulation with diC8-PIP_3 produced no detectable signal (Fig. 2A–B). However, chronic stimulation with diC8-PIP_3 led to a significant increase in $PI(3,4)P_2$ in the plasma membrane (Fig. 2C). These data suggest that diC8-PIP_3 partitions slowly across the cell membrane, where it is efficiently converted to diC8-$PI(3,4)P_2$. We could not detect increases in plasma membrane $PI(3,4)P_2$ after chronic incubation of cells with diC8- $PI(3,4)P_2$.

In a parallel approach, we tested whether the rescue of gelatin degradation by diC8-lipids required SHIP2. We first treated cells with the SHIP2 inhibitor AS1949490, which blocked gelatin degradation in MDA-MB-231 cells (Fig. 3A). Gelatin degradation in AS1949490-treated cells was rescued by diC8-$PI(3,4)P_2$, but not diC8-PIP_3, showing that PIP_3 cannot

drive matrix degradation in the absence of SHIP2 activity. Similarly, we treated cells with PTX to block PI3Kβ activation and inhibit gelatin degradation (Fig. 3B). While gelatin degradation was rescued by diC8-PIP_3, this rescue was abrogated when cells were co-treated with the SHIP2 inhibitor AS1949490 (Fig. 3B). Together, these results suggest that diC8-PIP_3 must be converted to diC8-$PI(3,4)P_2$ to rescue invadopodia activity and gelatin degradation.

Activating PIK3CB and PIK3CA mutants rescue gelatin degradation in cells treated with PTX.

To increase cellular PIP_3 levels using an orthogonal approach, we next tested whether expression of the constitutively active p110β mutants D1067Y (20) or E1051K (21) would rescue gelatin degradation in PTX-treated cells. Stable expression of the mutants in MDA-MB-231 cells led to robust Akt activation (Fig. 4A, 4B), demonstrating that the p110β mutants increased PI3K signaling. Similarly, increases in both $PI(3,4)P_2$ and PIP_3 could be detected using fluorescent biosensors in cells expressing mutant p110β (Fig. 4C). Whereas treatment of control MDA-MB-231 cells with PTX reduced gelatin degradation, cells expressing the E1051K and D1067Y activating mutations were unaffected by PTX (Fig. 4D).

The ability of diC8-PIP_3 to rescue gelatin degradation in TGX221-treated cells (Fig. 1B) suggested that rescue by constitutively active PI3Kβ mutants might not be isotype selective. We therefore stably expressed wild type or constitutively active (H1047R and E545K) p110α in MDA-MB-231 cells (22). Overexpression of both mutants led to increased Akt activation (Fig. 5A–B). An increase in plasma membrane PIP_3 and $PI(3,4)P_2$ were also detected with the H1047R mutant, although not with the E545K mutant (Fig. 4C); the reason for this difference is not clear but could reflect differential signaling by the two mutants (22). Expression of H1047R but not wild type p110α overcame the inhibition of gelatin degradation by PTX (Fig. 5C). Similarly, TGX221 failed to inhibit gelatin degradation in cells overexpressing either wild type or H1047R-p110α (Fig. 5E). Consistent with our data with C8-lipids (Fig. 3), gelatin degradation in cells expressing E545K-p110α were unaffected by PTX but was blocked by treatment of cells with the SHIP2 inhibitor (Fig. 6).

Discussion

Our data, along with published work from other labs, support a model in which invadopodial maturation requires the SHIP2-dependent conversion of PIP_3 to $PI(3,4)P_2$ (15–17). We have also previously shown that the PI3Kβ isotype is selectively required for production of $PI(3,4)P_2$ in invadopodia (7). The mechanism for coupling between PI3Ks and SHIP2 is not known. PI3Kβ binds to CRKL in PTEN-deficient tumor cells (23). This could recruit PI3Kβ to integrin-associated scaffolds such as p130Cas (24) and Nedd9 (25), which also bind to SHIP2 (24,26). Alternatively, independent of its localization, PI3Kβ could be preferentially activated during matrix degradation, to produce more PIP_3 than other isotypes. In neutrophils, PIP_3 production by PI3Kβ exceeds that of other Class I PI3Ks under conditions of maximal activity (resulting from simultaneous RTK and GPCR activation) (9). Integrins are known to couple to tyrosine kinases that lead to activation of PI3K (27–29),

and we have shown a requirement for Gβγ binding to PI3Kβ during invadopodia maturation (7,16). These data suggest that PI3Kβ in invadopodia could be subject to a maximally activating combined RTK/GPCR stimulus.

Despite the mechanism for selective PI3Kβ-SHIP2 coupling in tumor cells, this selectivity can be overcome when PIP_3 levels are increased by pharmacological treatments or mutational pathway activation. Our data show that the reduction in gelatin degradation caused by PTX or TGX221 treatment is rescued by the addition of diC8-PI(3,4)P_2 or -PIP_3, or by expression of constitutively active PI3Kβ or PI3Kα. Consistent with our earlier results (7), rescue by either method is dependent on SHIP2 activity.

The behavior of diC8 lipids in cells is not fully understood. Acute addition of either diC8-PIP_3 or diC8-PI(3,4)P_2 has no detectable effect on the recruitment of PH domain probes to the membrane, suggesting that they do not rapidly reach the cell interior. In contrast, 18 h treatment of PIP_3 led to a significant increase in plasma membrane PI(3,4)P_2. This observation suggests that diC8-PIP_3 partitions slowly into the inner leaflet of the plasma membrane, where it is converted to diC8-PI(3,4)P_2. While we were unable to detect the appearance of diC8-PI(3,4)P_2 after an 18 h incubation, the lipids clearly accumulate to levels sufficient to promote invadopodia function, as it rescues gelatin degradation in cells treated with PTX or the PI3Kβ inhibitor TGX221. It is unlikely that the effects of diC8-PI(3,4)P_2 on matrix degradation are due to its conversion to diC8-PI(3)P and diC8-PI(4)P. While MDA-MB-231 cells do not express INPP4B, which hydrolyzes PI(3,4)P_2 to PI(3)P (30), they do express PTEN, which hydrolyzes PI(3,4)P_2 to PI(4)P (31,32). However, knockdown of PI4KIIα has no effect on invadopodia and knockdown PI4KIIβ induces invadopodia (33). Finally, it is also possible that the effective lifetime of diC8-PI(3,4)P_2 is longer in MDA-MB-231 than in HEK293A cells due to lack of INPP4B in MDA-mB-231 cells (30).

Our previously published data suggest that PI3Kβ inhibitors might be useful to inhibit tumor cell invasion during metastasis (7,16). Our study suggests that activating mutations of PIK3CA might bypass the requirement for PI3Kβ in invadopodia, by elevating PIP_3 levels and PIP_3 conversion to PI(3,4)P_2. This is analogous to the loss of PI3Kβ-dependent growth in PTEN-null tumors that also express mutations that activate PI3Kα (34). These experiments highlight the importance of determining the genetic features of a tumor to develop effective therapeutics against tumor metastasis.

Material and Methods

Antibodies and Reagents

Antibodies to GAPDH (2118), p110β (3011), p110α (4249), pS473-Akt (4060) and total Akt (9272) were purchased from Cell Signaling Technology. Rhodamine-phalloidin (R415) was purchased from Invitrogen. Poly-L-lysine (0.01%; P4707) and gelatin from porcine skin type A (G2625) was purchased from Sigma. Glutaraldehyde was purchased from Electron Microscopy Sciences. Formaldehyde was purchased from Invitrogen. DAPI Fluoromount-G was purchased from Southern Biotech and was used for mounting coverslips. TGX221 was purchased from Selleckchem. AS1949490 was purchased from Sigma. Pertussis toxin was purchased from Millipore. Oregon Green-488 conjugated gelatin (G13186) was purchased

from Invitrogen. diC8-PI(3,4)P_2, (P3408), diC8-PIP_3 (P3908), and diC8-PI(3,5)P_2 (P3508) were purchased from Echelon Biosciences and were reconstituted in sterile water to a final concentration of 1 mM.

Cell Culture

The human breast cancer cell line MDA-MB-231 was obtained from the American Type Culture Collection. MDA-MB-231 cells were cultured in DMEM containing 10% fetal bovine serum at 37 °C and 5% CO_2. Lentivirus infected cell lines were maintained in 2 μg/ml puromycin.

DNA constructs, Virus production, and Transductions

MDA-MB-231 cells overexpressing wild type or constitutively active PIK3CA were described previously (22). pHAGE-PIK3CB-E1051K (116553), pHAGE-PIK3CB-D1067Y (116551), and helper and packaging constructs pMD2.6 (23359) and psPAX2 (12260) were purchased from Addgene. Lentiviruses were produced by transfecting HEK293T cells with the PIK3CB constructs along with pMD2.6 and psPAX2 using Lipofectamine 3000 (Invitrogen). After 24 h, viral supernatants were filtered with a 0.45 μm filter. MDA-MB-231 cells were infected with virus and selected with puromycin (4 μg/ml). Expression of p110β was verified by western blot. For cell lines expressing constitutively active PI3K, activation was evaluated by measuring pS473-Akt.

Western Blotting

Cells were plated on 60 mm gelatin coated tissue culture dishes. The tissue culture dishes were coated with 0.01% poly-L-lysine for 10 minutes at room temperature and then washed three times with PBS. The dishes were treated with 0.5% glutaraldehyde for 10 minutes, washed 5 times with PBS, and then incubated with 0.2% gelatin diluted in PBS for 30 minutes at 37 °C. The dishes were then treated with 0.1M glycine for 10 minutes at room temperature, washed twice with PBS, and then seeded with cells. Cells were lysed in Laemmli buffer lacking bromophenol blue and supplemented with 100 μM PMSF, 1 μg/ml leupeptin, 1 μg/ml aprotinin, 1 mM DTT, and 1:100 phosphatase inhibitor cocktails 2 (P5726) and 3 (P0044) from Sigma. Cell lysates were boiled for 5 minutes at 100 °C and sonicated. Protein concentrations were determined using the Bio-Rad DC protein assay kit. 30 μg of lysate was mixed with Laemmli sample buffer containing 200 mM DTT, boiled at 100 °C for 5 minutes, and analyzed by SDS-PAGE and western blotting with the Super Signal West Pico PLUS Chemiluminescent Substrate (Thermo-Scientific). Gels were imaged using a Kodak Image Station 4000R.

Gelatin Degradation Assay

The gelatin degradation assay was performed as described previously (16). In brief, acid-washed coverslips were coated with 0.01% poly-L-lysine, cross-linked with 0.5% glutaraldehyde, coated with 200 μg/ml Oregon Green 488-conjugated gelatin for 15 min and quenched with 0.1M glycine. For experiments with diC8 lipids (1 μM) or inhibitors (500 nM TGX221 or 10 μM AS1949490), cells were pretreated for 30 minutes before seeding. For experiments using PTX (200 ng/ml), cells were pre-treated for 15 h before seeding. 8.5×10^4

cells were seeded on Oregon Green 488-conjugated gelatin coated coverslips, incubated for 18 h in the presence of lipids or inhibitors, fixed with 4% formaldehyde and permeabilized with 0.05% Triton X-100. Cells were stained with Rhodamine-phalloidin, and mounted using Dapi Fluoromount-G. For the gelatin degradation assay, images were acquired with a 60× 1.4 NA objective on a Nikon Eclipse E400 microscope. For quantification of the fluorescent gelatin images, the background was subtracted with a rolling ball radius of 20. The images were thresholded to define areas of degradation per cell, which was measured in ImageJ.

Live-cell imaging of diC$_8$-lipid loaded cells

HEK293A cells (RRID:CVCL_6910) grown in DMEM supplemented with 10% fetal bovine serum, 100 u/ml penicillin, 10 μg/ml streptomycin and 0.1% chemically-defined lipid supplement(ThermoFisher) were seeded into #1.5 22 mm diameter glass-bottom 35 mm dishes (CellVis) coated with 20 μg/ml entactin-collagen-laminin mix. At least 1 hour post-seeding, cells were transfected with 0.8 μg mNeonGreen-cPHx3 and 0.2 μg mCherry-aPHx2 plasmids pre-incubated for > 5 min with 3 μg lipofectamine 2000 in 200 μl Opti-MEM. Transfection media was replaced after 3–4 hours with Fluorobrite medium (ThermoFisher) supplemented with 0.1% BSA and 0.1% chemically-defined lipid supplement. As indicated in the figure, EGF or diC$_8$ lipids were added to 20 ng/ml or 1 μM, respectively. Immediately prior to imaging, cells were stained with the selective plasma membrane dye Cell Mask Deep Red at 1 μg/ml for 5 min before rinsing. Imaging was performed 24 hours post transfection on a Nikon A1R resonant scanning confocal microscope using a 1.45 NA, 100x plan-apochromatic objective lens mounted on a Nikon Ti inverted microscope stand. The confocal pinhole was set to acquire at a resolution of 1.2 airy units on the far-red channel. Green (mNeonGreen), red (mCherry) and far red (Cell Mask) fluorescence were excited with 488 nm, 561 nm and 640 nm diode lasers on sequential scans and detected on separate photomultiplier tubes equipped with appropriate dichroic and emission optics (500–550 nm for green, 570–620 nm for red, 663–737 nm for far red).

Image Analysis.—Images saved in Nikon .nd2 format were opened using the LOCI bioformats importer for Fiji. Cell specific regions of interest (ROI) were drawn around whole cells and on small regions of cytoplasm. The Cell Mask channel was used to define a mask of the plasma membrane using an auto thresholding approach, based on wavelet decompositions across three wavelength-defined length scales as detailed in (35). Next, the masked region of plasma membrane in the green and red channels was normalized to the intensity of the cytoplasmic ROI in the same cells, defining the PM:Cyto ratio. This ratio was measured for each cell across all recorded time points.

Statistical analysis

All statistical analyses were performed using Graphpad Prism version 8. Statistical analyses were designed in consultation with the Einstein Biostatistics core. If the primary data, or the log2 transformation was normally distributed, a t-test or ANOVA was used. If the data was not normally distributed and a Kruska-Wallis test produced a significant result, p-values were generated using the Mann-Whitney U test.

Acknowledgments

This work was supported by DOD grant BC181067 (JMB), T32 GM7288 (CTJ) and NIGMS 1R35GM119412 (GRVH).

Data Availability:

Raw data, cell lines, and plasmids are available by contacting the corresponding author.

Abbreviations

DiC8	di-octanoyl
ECM	Extracellular Matrix
EGF	Epidermal Growth Factor
GPCR	G protein coupled receptors
PH domain	Pleckstrin homology domain
PI3K	Phosphoinositide 3-kinase
PI4KIIβ	Phosphatidylinositol 4-kinsae Type 2 Beta
PIP_3	Phosphatidylinositol (3,4,5)-triphosphate
PI(3)P	Phosphatidylinositol 3-phosphate
$PI(3,4)P_2$	Phosphatidylinositol (3,4)-diphosphate
$PI(3,5)P_2$	Phosphatidylinositol (3,5)-diphosphate
$PI(4,5)P_2$	Phosphatidylinositol (4,5)-diphosphate
PTX	Pertussis Toxin
RTK	Receptor Tyrosine Kinase
SYNJ2	Synaptojanin-2

References

1. Leong HS, Robertson AE, Stoletov K, Leith SJ, Chin CA, Chien AE, Hague MN, Ablack A, Carmine-Simmen K, McPherson VA, Postenka CO, Turley EA, Courtneidge SA, Chambers AF, and Lewis JD (2014) Invadopodia are required for cancer cell extravasation and are a therapeutic target for metastasis. Cell Rep 8, 1558–1570 [PubMed: 25176655]
2. Beaty BT, Sharma VP, Bravo-Cordero JJ, Simpson MA, Eddy RJ, Koleske AJ, and Condeelis J (2013) β1 integrin regulates Arg to promote invadopodial maturation and matrix degradation. Molecular biology of the cell 24, 1661–1675 [PubMed: 23552693]
3. Eddy RJ, Weidmann MD, Sharma VP, and Condeelis JS (2017) Tumor cell invadopodia: invasive protrusions that orchestrate metastasis. Trends in cell biology 27, 595–607 [PubMed: 28412099]
4. Murphy DA, and Courtneidge SA (2011) The'ins' and'outs' of podosomes and invadopodia: characteristics, formation and function. nature reviews molecular cell biology 12, 413 [PubMed: 21697900]

5. Branch KM, Hoshino D, and Weaver AM (2012) Adhesion rings surround invadopodia and promote maturation. Biol Open 1, 711–722 [PubMed: 23213464]
6. Beaty BT, and Condeelis J (2014) Digging a little deeper: the stages of invadopodium formation and maturation. Eur J Cell Biol 93, 438–444 [PubMed: 25113547]
7. Erami Z, Heitz S, Bresnick AR, and Backer JM (2019) PI3Kbeta links integrin activation and PI(3,4)P2 production during invadopodial maturation. Mol Biol Cell, mbcE19030182
8. Yamaguchi H, Yoshida S, Muroi E, Yoshida N, Kawamura M, Kouchi Z, Nakamura Y, Sakai R, and Fukami K (2011) Phosphoinositide 3-kinase signaling pathway mediated by p110alpha regulates invadopodia formation. J Cell Biol 193, 1275–1288 [PubMed: 21708979]
9. Houslay DM, Anderson KE, Chessa T, Kulkarni S, Fritsch R, Downward J, Backer JM, Stephens LR, and Hawkins PT (2016) Coincident signals from GPCRs and receptor tyrosine kinases are uniquely transduced by PI3Kβ in myeloid cells. Sci. Signal 9, ra82–ra82 [PubMed: 27531651]
10. Burke JE, and Williams RL (2015) Synergy in activating class I PI3Ks. Trends Biochem Sci 40, 88–100 [PubMed: 25573003]
11. Bresnick AR, and Backer JM (2019) PI3Kβ–a versatile transducer for GPCR, RTK and small GTPase signaling. Endocrinology
12. Thorpe LM, Yuzugullu H, and Zhao JJ (2015) PI3K in cancer: divergent roles of isoforms, modes of activation and therapeutic targeting. Nat Rev Cancer 15, 7–24 [PubMed: 25533673]
13. Suwa A, Kurama T, and Shimokawa T (2010) SHIP2 and its involvement in various diseases. Expert opinion of therapeutic targets 14, 727–737
14. Ben-Chetrit N, Chetrit D, Russell R, Korner C, Mancini M, Abdul-Hai A, Itkin T, Carvalho S, Cohen-Dvashi H, Koestler WJ, Shukla K, Lindzen M, Kedmi M, Lauriola M, Shulman Z, Barr H, Seger D, Ferraro DA, Pareja F, Gil-Henn H, Lapidot T, Alon R, Milanezi F, Symons M, Ben-Hamo R, Efroni S, Schmitt F, Wiemann S, Caldas C, Ehrlich M, and Yarden Y (2015) Synaptojanin 2 is a druggable mediator of metastasis and the gene is overexpressed and amplified in breast cancer. Sci Signal 8, ra7 [PubMed: 25605973]
15. Sharma VP, Eddy R, Entenberg D, Kai M, Gertler FB, and Condeelis J (2013) Tks5 and SHIP2 regulate invadopodium maturation, but not initiation, in breast carcinoma cells. Current Biology 23, 2079–2089 [PubMed: 24206842]
16. Khalil BD, Hsueh C, Cao Y, Saab WFA, Wang Y, Condeelis JS, Bresnick AR, and Backer JM (2016) GPCR signaling mediates tumor metastasis via PI3Kβ. Cancer Research, canres. 1675.2015
17. Ghosh S, Scozzaro S, Ramos AR, Delcambre S, Chevalier C, Krejci P, and Erneux C (2018) Inhibition of SHIP2 activity inhibits cell migration and could prevent metastasis in breast cancer cells. J Cell Sci 131
18. Viaud J, Lagarrigue F, Ramel D, Allart S, Chicanne G, Ceccato L, Courilleau D, Xuereb JM, Pertz O, Payrastre B, and Gaits-Iacovoni F (2014) Phosphatidylinositol 5-phosphate regulates invasion through binding and activation of Tiam1. Nat Commun 5, 4080 [PubMed: 24905281]
19. Goulden BD, Pacheco J, Dull A, Zewe JP, Deiters A, and Hammond GRV (2019) A high-avidity biosensor reveals plasma membrane PI(3,4)P2 is predominantly a class I PI3K signaling product. J Cell Biol 218, 1066–1079 [PubMed: 30591513]
20. Nakanishi Y, Walter K, Spoerke JM, O'Brien C, Huw LY, Hampton GM, and Lackner MR (2016) Activating Mutations in PIK3CB Confer Resistance to PI3K Inhibition and Define a Novel Oncogenic Role for p110beta. Cancer Res 76, 1193–1203 [PubMed: 26759240]
21. Whale AD, Colman L, Lensun L, Rogers HL, and Shuttleworth SJ (2017) Functional characterization of a novel somatic oncogenic mutation of PIK3CB. Signal Transduct Target Ther 2, 17063 [PubMed: 29279775]
22. Pang H, Flinn R, Patsialou A, Wyckoff J, Roussos ET, Wu H, Pozzuto M, Goswami S, Condeelis JS, Bresnick AR, Segall JE, and Backer JM (2009) Differential enhancement of breast cancer cell motility and metastasis by helical and kinase domain mutations of class IA phosphoinositide 3-kinase. Cancer Res 69, 8868–8876 [PubMed: 19903845]
23. Zhang J, Gao X, Schmit F, Adelmant G, Eck MJ, Marto JA, Zhao JJ, and Roberts TM (2017) CRKL mediates p110β-dependent PI3K signaling in PTEN-deficient cancer cells. Cell Reports 20, 549–557 [PubMed: 28723560]

24. Prasad N, Topping RS, and Decker SJ (2001) SH2-containing inositol 5′-phosphatase SHIP2 associates with the p130Cas adapter protein and regulates cellular adhesion and spreading. Molecular cellular biology 21, 1416–1428 [PubMed: 11158326]
25. Hamze-Komaiha O, Sarr S, Arlot-Bonnemains Y, Samuel D, and Gassama-Diagne A (2016) SHIP2 Regulates Lumen Generation, Cell Division, and Ciliogenesis through the Control of Basolateral to Apical Lumen Localization of Aurora A and HEF 1. Cell Rep 17, 2738–2752 [PubMed: 27926875]
26. Chodniewicz D, and Klemke RL (2004) Regulation of integrin-mediated cellular responses through assembly of a CAS/Crk scaffold. Bba-Mol Cell Res 1692, 63–76
27. King WG, Mattaliano MD, Chan TO, Tsichlis PN, and Brugge JS (1997) Phosphatidylinositol 3-kinase is required for integrin-stimulated AKT and Raf-1/mitogen-activated protein kinase pathway activation. Mol Cell Biol 17, 4406–4418 [PubMed: 9234699]
28. Manganaro D, Consonni A, Guidetti GF, Canobbio I, Visconte C, Kim S, Okigaki M, Falasca M, Hirsch E, Kunapuli SP, and Torti M (2015) Activation of phosphatidylinositol 3-kinase beta by the platelet collagen receptors integrin alpha2beta1 and GPVI: The role of Pyk2 and c-Cbl. Bba-Mol Cell Res 1853, 1879–1888
29. Genna A, Lapetina S, Lukic N, Twafra S, Meirson T, Sharma VP, Condeelis JS, and Gil-Henn H (2018) Pyk2 and FAK differentially regulate invadopodia formation and function in breast cancer cells. J Cell Biol 217, 375–395 [PubMed: 29133485]
30. Fedele CG, Ooms LM, Ho M, Vieusseux J, O'Toole SA, Millar EK, Lopez-Knowles E, Sriratana A, Gurung R, Baglietto L, Giles GG, Bailey CG, Rasko JE, Shields BJ, Price JT, Majerus PW, Sutherland RL, Tiganis T, McLean CA, and Mitchell CA (2010) Inositol polyphosphate 4-phosphatase II regulates PI3K/Akt signaling and is lost in human basal-like breast cancers. Proc Natl Acad Sci U S A 107, 22231–22236 [PubMed: 21127264]
31. Malek M, Kielkowska A, Chessa T, Anderson KE, Barneda D, Pir P, Nakanishi H, Eguchi S, Koizumi A, Sasaki J, Juvin V, Kiselev VY, Niewczas I, Gray A, Valayer A, Spensberger D, Imbert M, Felisbino S, Habuchi T, Beinke S, Cosulich S, Le Novere N, Sasaki T, Clark J, Hawkins PT, and Stephens LR (2017) PTEN Regulates PI(3,4)P2 Signaling Downstream of Class I PI3K. Mol Cell 68, 566–580 e510 [PubMed: 29056325]
32. Reed DE, and Shokat KM (2017) INPP4B and PTEN Loss Leads to PI-3,4-P2 Accumulation and Inhibition of PI3K in TNBC. Mol Cancer Res 15, 765–775 [PubMed: 28196852]
33. Alli-Balogun GO, Gewinner CA, Jacobs R, Kriston-Vizi J, Waugh MG, and Minogue S (2016) Phosphatidylinositol 4-kinase IIbeta negatively regulates invadopodia formation and suppresses an invasive cellular phenotype. Mol Biol Cell 27, 4033–4042 [PubMed: 27798239]
34. Schmit F, Utermark T, Zhang S, Wang Q, Von T, Roberts TM, and Zhao JJ (2014) PI3K isoform dependence of PTEN-deficient tumors can be altered by the genetic context. Proc Natl Acad Sci U S A 111, 6395–6400 [PubMed: 24737887]
35. Wills RC, Pacheco J, and Hammond GRV (2021) Quantification of Genetically Encoded Lipid Biosensors. Methods Mol Biol 2251, 55–72 [PubMed: 33481231]

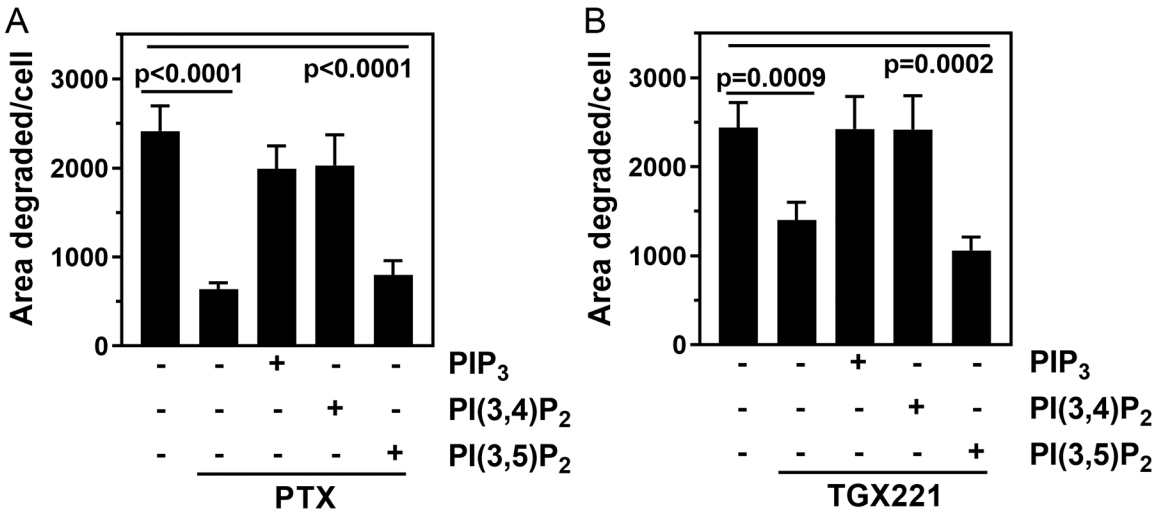

Figure 1: diC8-PIP_3 and diC8-$PI(3,4)P_2$ rescue gelatin degradation in PTX and TGX treated MDA-MB-231 cells.

A) Gelatin degradation was measured in parental MDA-MB-231 cells treated with PTX in the absence or presence of diC8-phosphoinositides. B) Gelatin degradation was measured in parental MDA-MB-231 cells treated with TGX221 in the absence or presence of diC8-PIP_3,-$PI(3,4)P_2$, or -$PI(3,5)P_2$. Data are the mean ± SEM from 4 or 3 independent experiments, respectively.

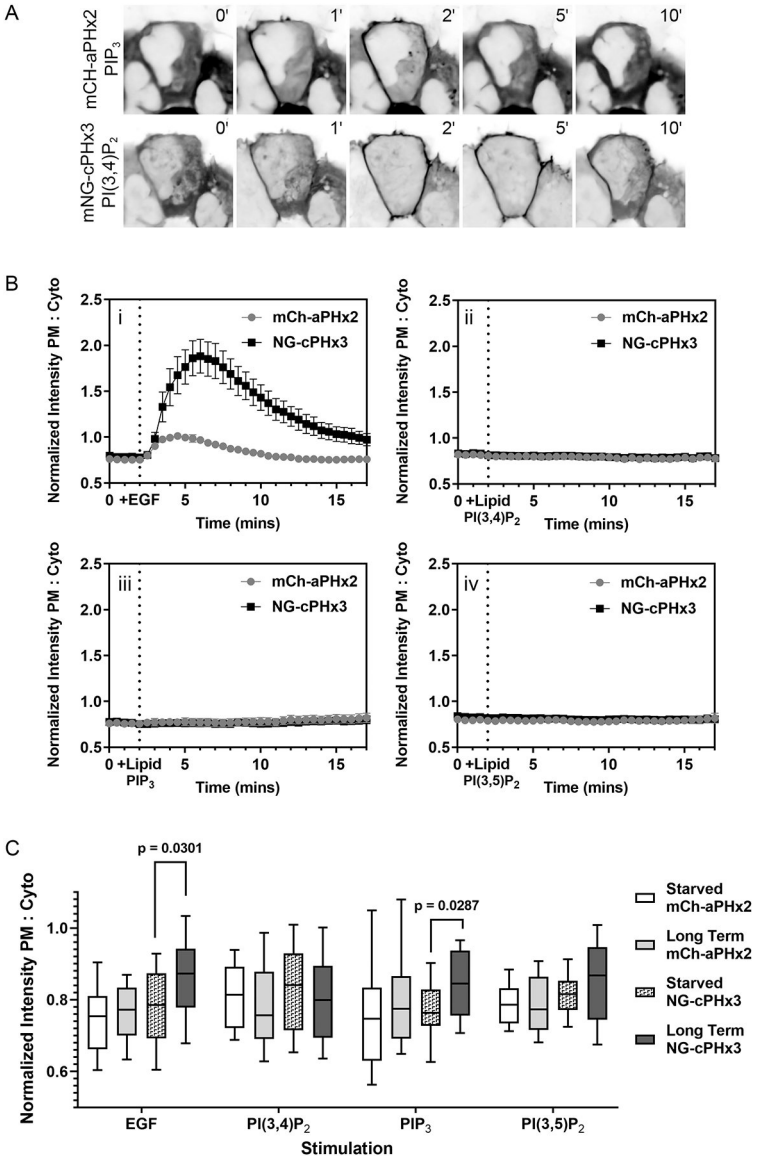

Figure 2: Treatment of cells with diC8-PIP_3 leads to an increase in plasma membrane $PI(3,4)P_2$.

HEK293A cells were transfected with reporters for $PI(3,4)P_2$ (mNeonGreen-cPHx3) or PIP_3 (mCherry-aPHx2). A) Representative images from time lapse movies of cells expressing the $PI(3,4)P_2$ and PIP_3 reporters and stimulated with EGF. B) Cells were treated with EGF or diC8-phosphoinositides for 15 min; images were taken every 30 s and stimuli were added after 2 min of imaging. The ratio of plasma membrane to cytosolic fluorescence intensity was calculated as described (19). The data are the mean ± SEM from 3 independent experiments, n = 29–34 cells. C) Cells were incubated with EGF or diC8-phosphoinositides for 15–22h. The ratio of plasma membrane to cytosolic fluorescence intensity was compared to data from Fig. 2A taken at 1 min, before the stimuli were added. P-values were obtained by Kruskal-Wallis tests using an alpha of 0.05. The data are pooled from 3 independent experiments, n = 31–35 cells.

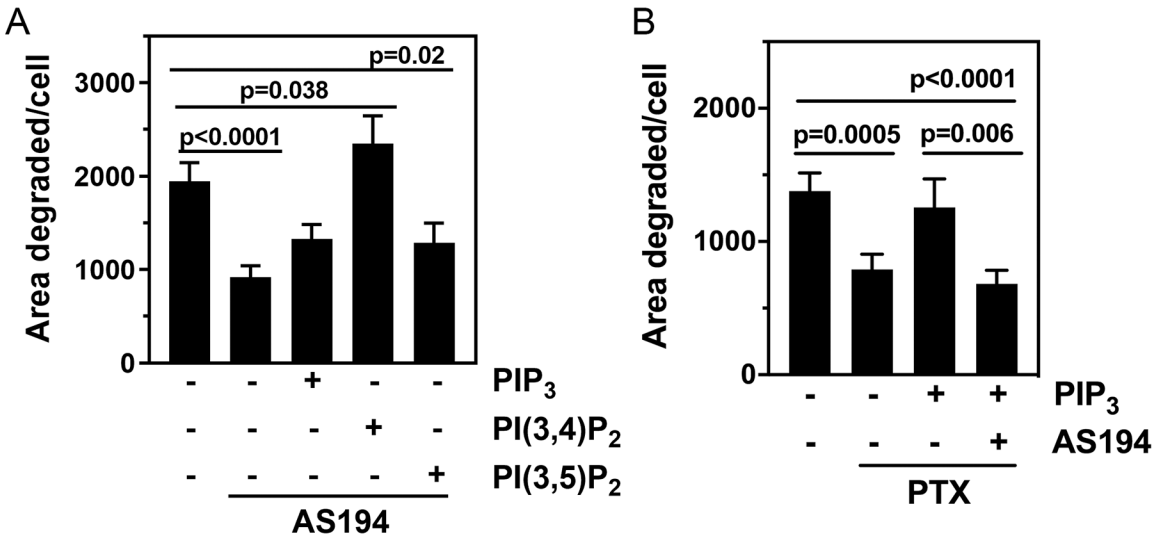

Figure 3: diC8-PI(3,4)P_2 but not diC8-PIP_3 rescues gelatin degradation in MDA-MB-231 cells treated with SHIP2 inhibitor.

A) Gelatin degradation was measured in parental MDA-MB-231 cells treated with AS1949490 in the absence or presence of diC8-phosphoinositides. B) Gelatin degradation was measured in parental MDA-MB-231 cells treated with PTX alone or co-treated with PTX and AS1949490, in the absence or presence of diC8-PIP_3. The data are the mean ± SEM from 3 independent experiments.

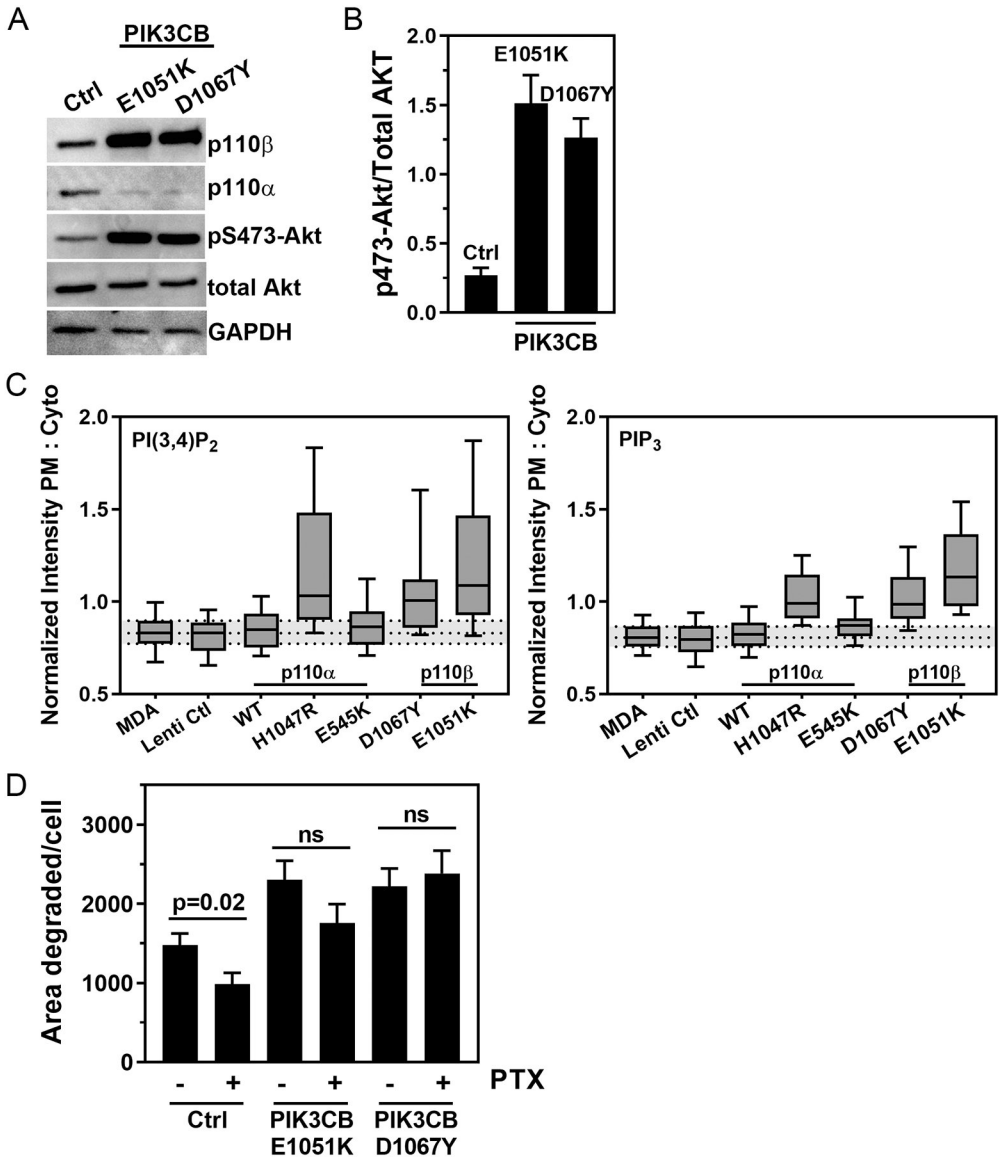

Figure 4: Activating PIK3CB mutants rescue gelatin degradation in PTX treated cells.

A) Lysates from lentivirus control MDA-MB-231 cells, or cells stably overexpressing E1051K or D1067Y p110β were blotted for p110β, p110α, pS473-AKT, total AKT, and GAPDH. B) Western blots were quantitated using a Kodak Image Station 4000R. The data are the mean ± SEM from 3 independent experiments. C) MDA-MB-231 cells stably expressing E1051K p110β, D1067Y p110β, E545K p110α or H1047R p110α were transfected with reporters for $PI(3,4)P_2$ (mNeonGreen-cPHx3) or PIP_3 (mCherry-aPHx2). The ratio of plasma membrane to cytosolic fluorescence intensity was calculated as described (19). The data are the mean ± SEM from 3 independent experiments, n = 49–58 cells. D) Gelatin degradation was measured in control, PIK3CB E1051K, and PIK3CB D1067Y MDA-MB-231 cells treated without or with PTX. The data are the mean ± SEM from 3 independent experiments.

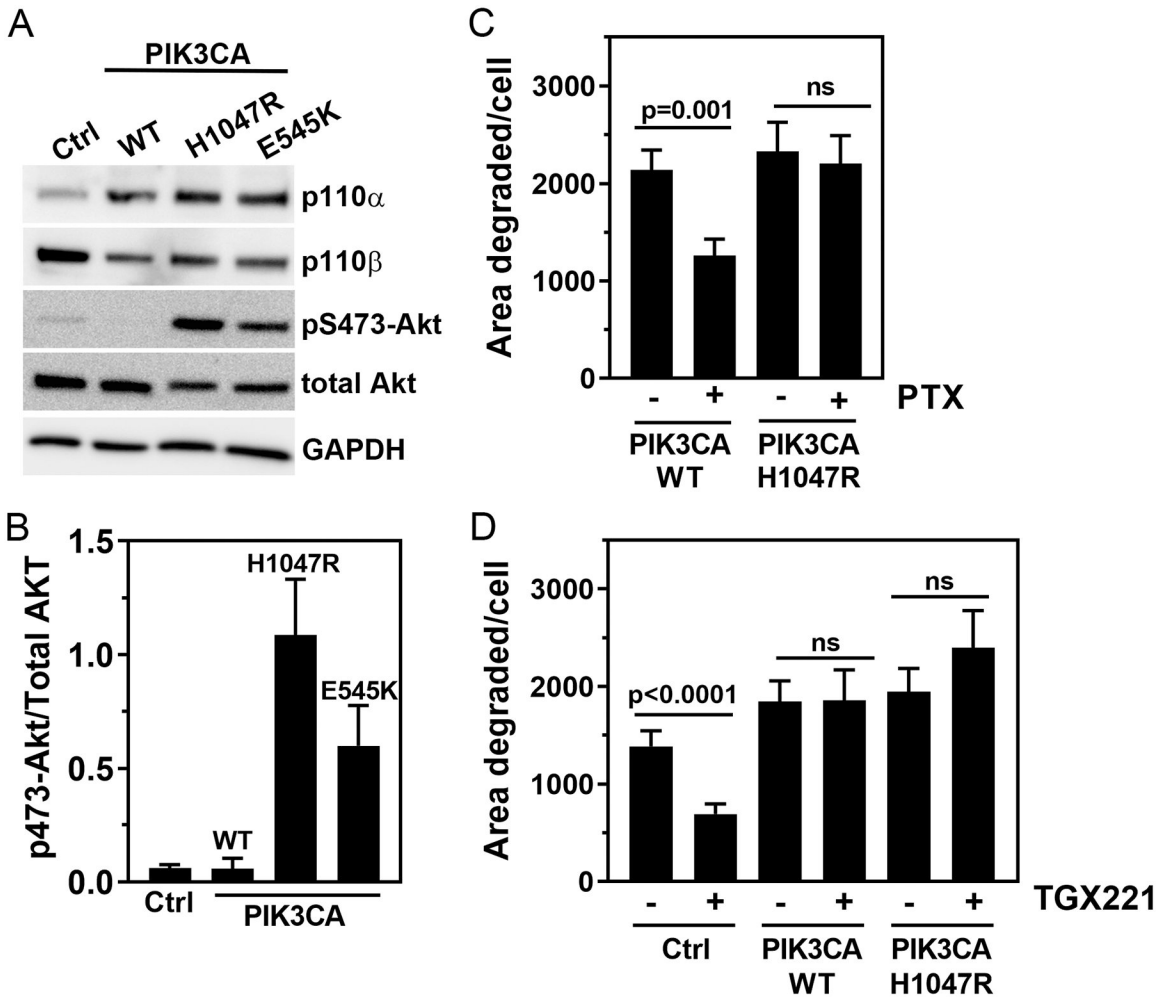

Figure 5: Activating PIK3CA mutation rescues gelatin degradation in PTX- and TGX221-treated cells.

A) Lysates from parental MDA-MB-231 cells or cells stably overexpressing WT, H1047R, or E545K p110α were blotted for p110β, p110α, pS473-AKT, total AKT, and GAPDH. B) Western blots were quantitated as above. The data are the mean ± SEM from 3 independent experiments. C) Gelatin degradation was measured in MDA-MB-231 cells overexpressing WT or H1047R p110α and treated with or without PTX. The data are the mean ± SEM from 3 independent experiments. D) Gelatin degradation was measured in parental MDA-MB-231 cells or cells overexpressing WT or H1047R p110α, and treated without or with TGX221. The data are the mean ± SEM from 3 independent experiments.

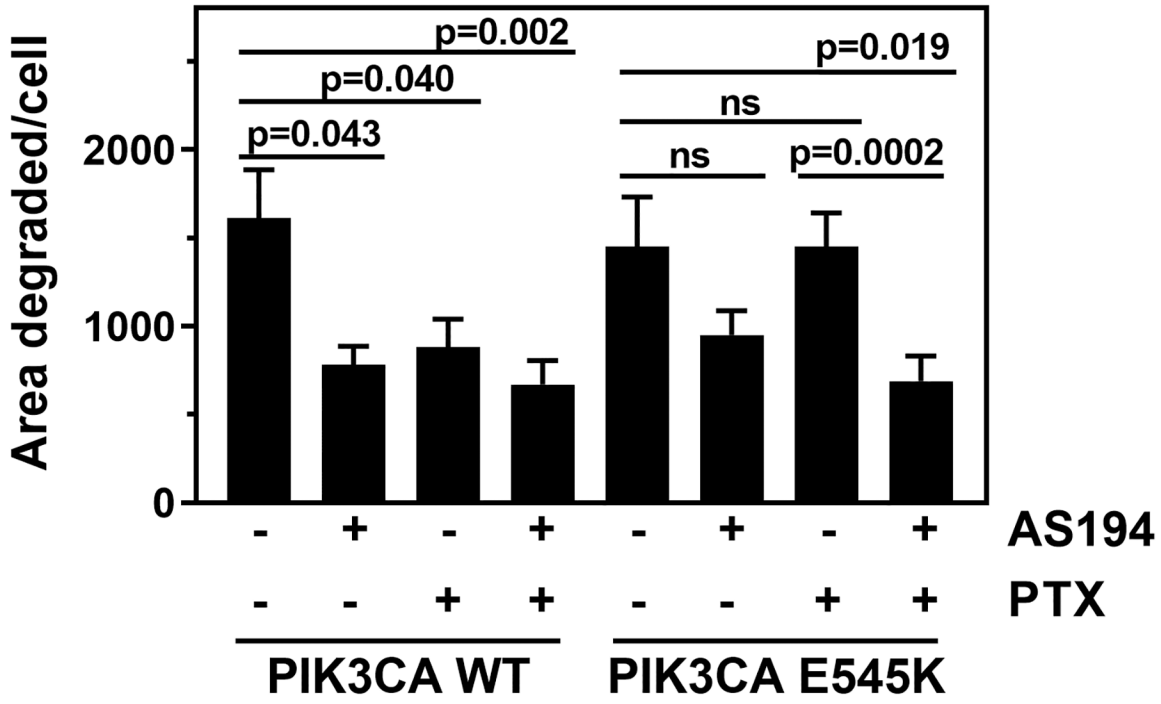

Figure 6: Rescue of gelatin degradation in PTX-treated cells by an activating PIK3CA mutant requires SHIP2 activity.

Gelatin degradation was measured in MDA-MB-231 cells overexpressing WT or E545K p110α and treated with PTX, AS1949490 or both. The data are the mean ± SEM from 2 independent experiments.